

# Supplementary Materials

## Photocatalytic Properties of Core-Shell Structured Wool-TiO<sub>2</sub> Hybrid Composite Powders

Haoshuai Gu<sup>1,2</sup>, Hui Zhang<sup>1,2,\*</sup>, Xinyue Zhang<sup>3</sup>, Yani Guo<sup>3</sup>, Limeng Yang<sup>1,2</sup>, Hailiang Wu<sup>2</sup>, and Ningtao Mao<sup>4,\*</sup>

<sup>1</sup> Research Centre for Functional Textile Materials, School of Textile Science and Engineering, Xi'an Polytechnic University, Xi'an, China; hsgu1117@163.com (H.G.); hzhangw532@xpu.edu.cn (H.Z.); yanglm@xpu.edu.cn (L.Y.)

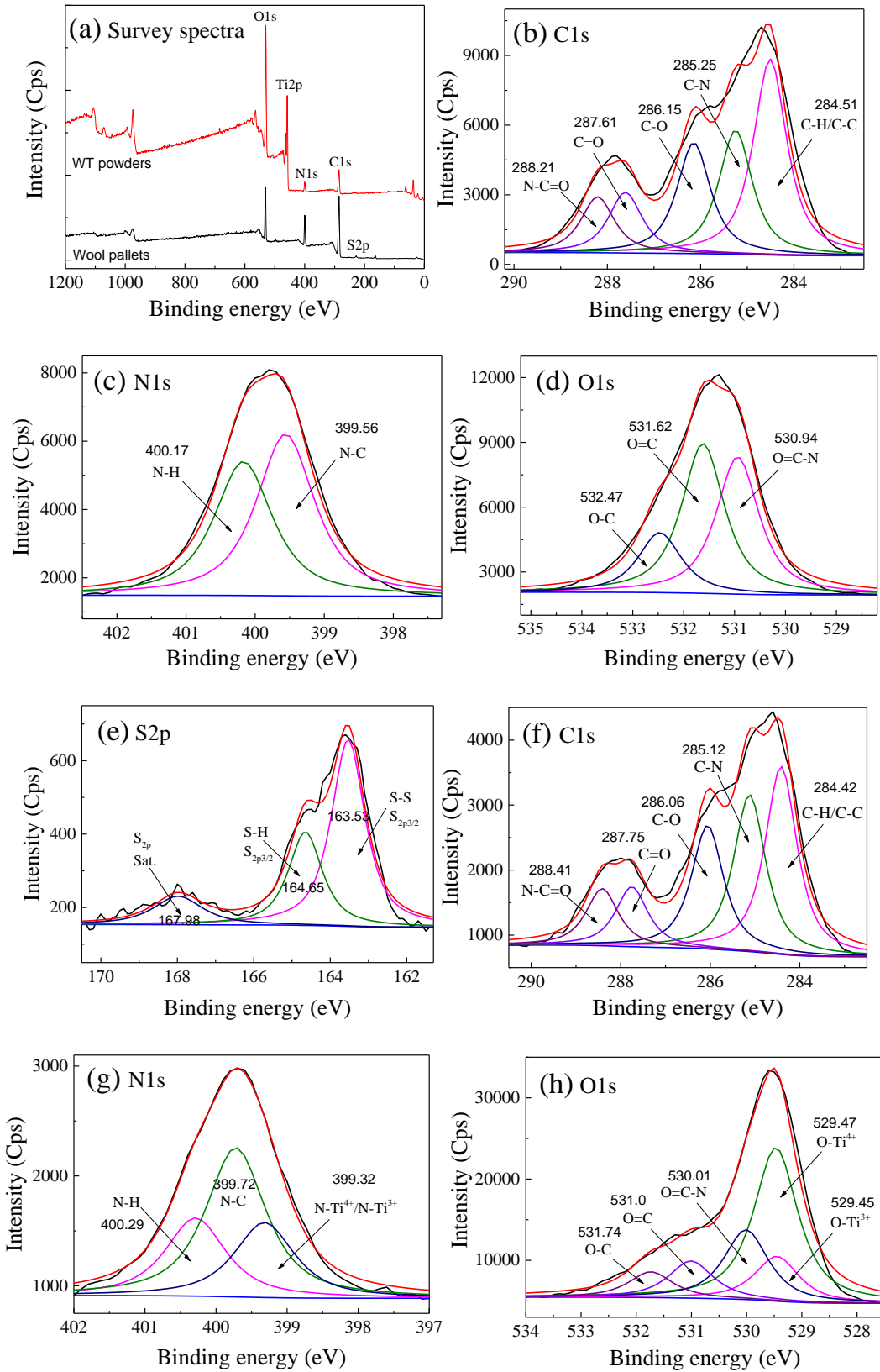
<sup>2</sup> Key Laboratory of Functional Textile Material and Product (Xi'an Polytechnic University), Ministry of Education, Xi'an, Shaanxi 710048, China; whl@xpu.edu.cn (H.W.)

<sup>3</sup> School of Environmental and Chemical Engineering, Xi'an Polytechnic University, Xi'an 710048, China; 41504040228@stu.xpu.edu.cn (X.Z.); 19940706@xpu.edu.cn (Y.G.)

<sup>4</sup> School of Design, University of Leeds, Leeds, LS2 9JT, United Kingdom; n.mao@leeds.ac.uk (N.M.)

\* Correspondence: hzhangw532@xpu.edu.cn (H.Z.); n.mao@leeds.ac.uk (N.M.)

**S1. XPS and FT-IR spectra of wool fibers, wool pallets and wool-TiO<sub>2</sub> (WT) hybrid composite powders**



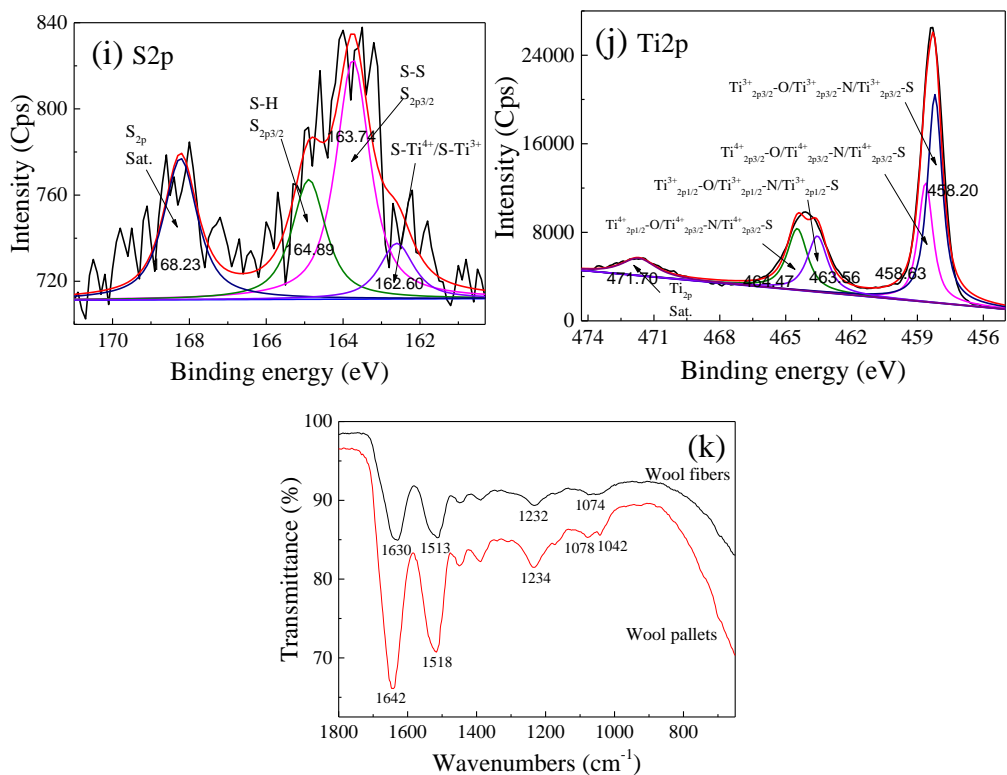


**Figure S1.** XPS spectra of wool pallets before and after loading TiO<sub>2</sub>: (a) survey spectra; wool pallets for (b) C1s, (c) N1s, (d) O1s, and (e) S2p; the WT powders for (f) C1s, (g) N1s, (h) O1s, (i) S2p, and (j) Ti2p; and (k) FT-IR spectra of wool fibers and wool pallets

## S2. The XPS elemental analysis data of the wool pallets and WT hybrid composite powders

**Table S1.** The XPS elemental analysis data

Samples	Peak	Position BE (eV)	FWHM (eV)	Atomic Concentration (%)
Wool pallets	C <sub>1s</sub>	284.80	2.42	62.93
	N <sub>1s</sub>	399.82	1.51	16.78
	O <sub>1s</sub>	531.82	1.89	18.68
	S <sub>2p</sub>	163.63	2.06	1.61
WT powders	C <sub>1s</sub>	284.80	2.37	25.82
	N <sub>1s</sub>	399.72	1.53	5.74
	O <sub>1s</sub>	529.55	1.33	47.56
	S <sub>2p</sub>	163.76	2.30	0.90
	Ti <sub>2p</sub>	458.32	1.12	19.98

## S3. The fitting data of the time-resolved PL spectra

**Table S2.** The fitting parameters of the time-resolved PL spectra using biexponential decay kinetics

Samples	$\tau_1$ (ns)	B <sub>1</sub> (%)	$\tau_2$ (ns)	B <sub>2</sub> (%)	$\tau_{\text{average}}$ (ns)	$\chi^2$
TiO <sub>2</sub> nanoparticles	0.47	0.522	/	0.0	/	1.191
WT powders	0.29	0.601	10.02	0.017	5.10	1.301

## S4. Optimization of the amount of TBT

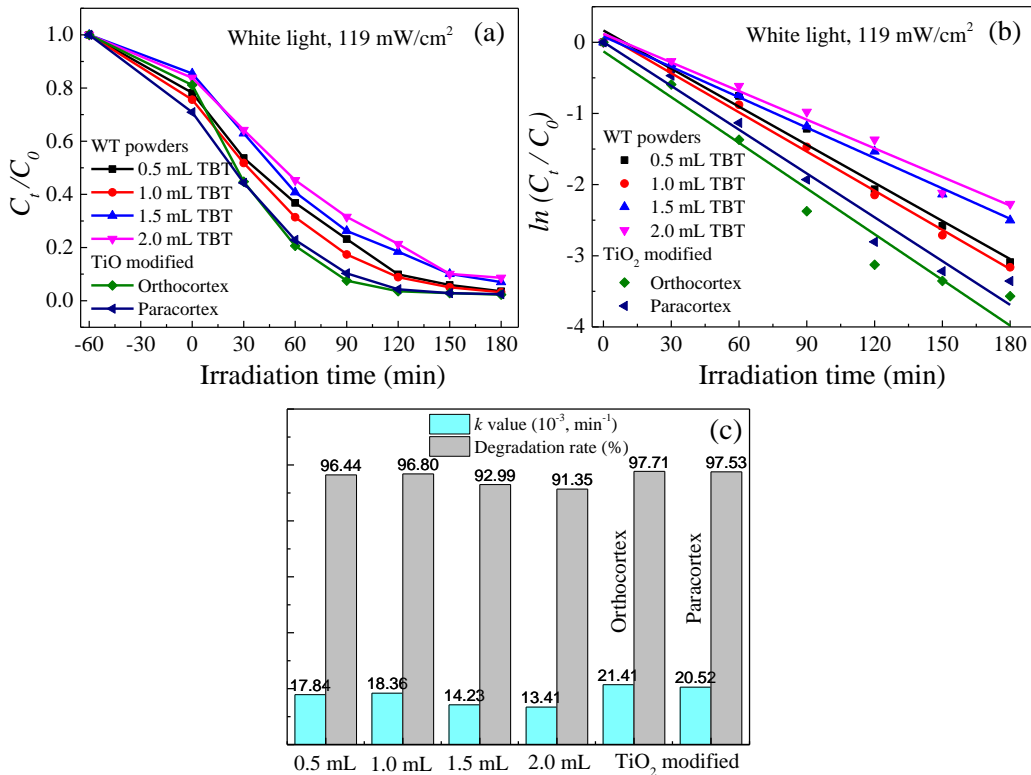


**Figure S2.** Photo-degradation of MB dye solutions exposed to white light at the light power density of  $119 \text{ mW/cm}^2$  for 180 min

### S5. Effect of the wavelength of light

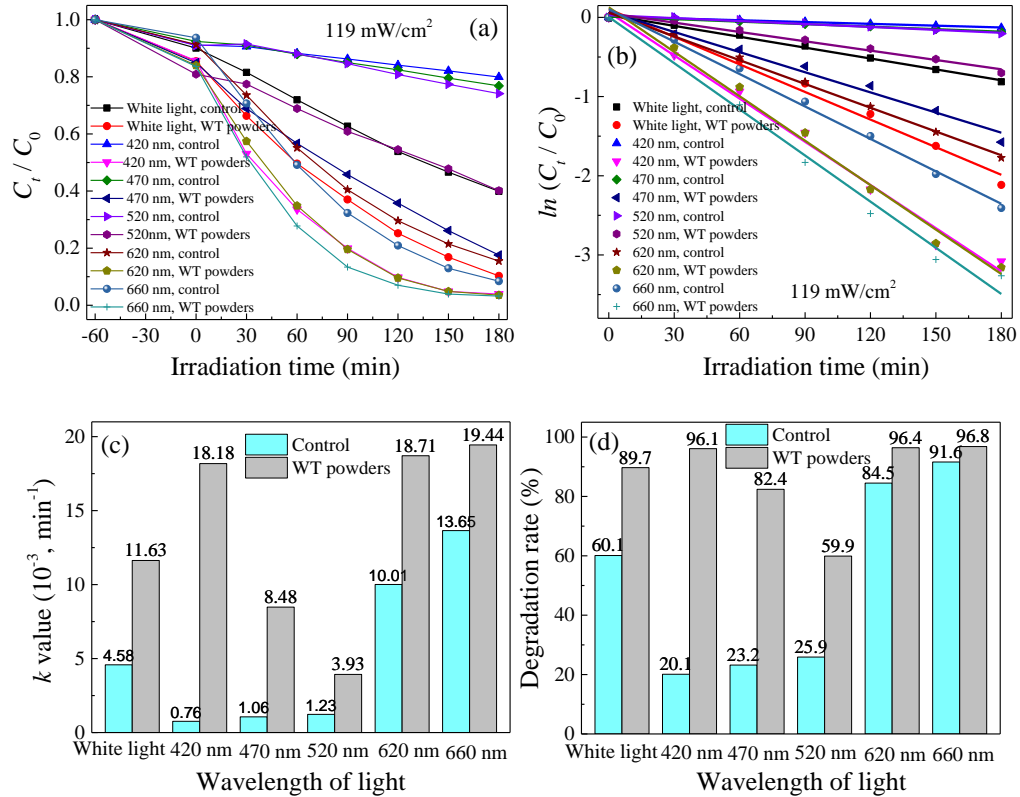


**Figure S3.** Photo-degradation of MB dye solution exposed to different wavelength lights at the light power density of  $119 \text{ mW/cm}^2$  for 180 min

### S6. Effect of the irradiation intensity

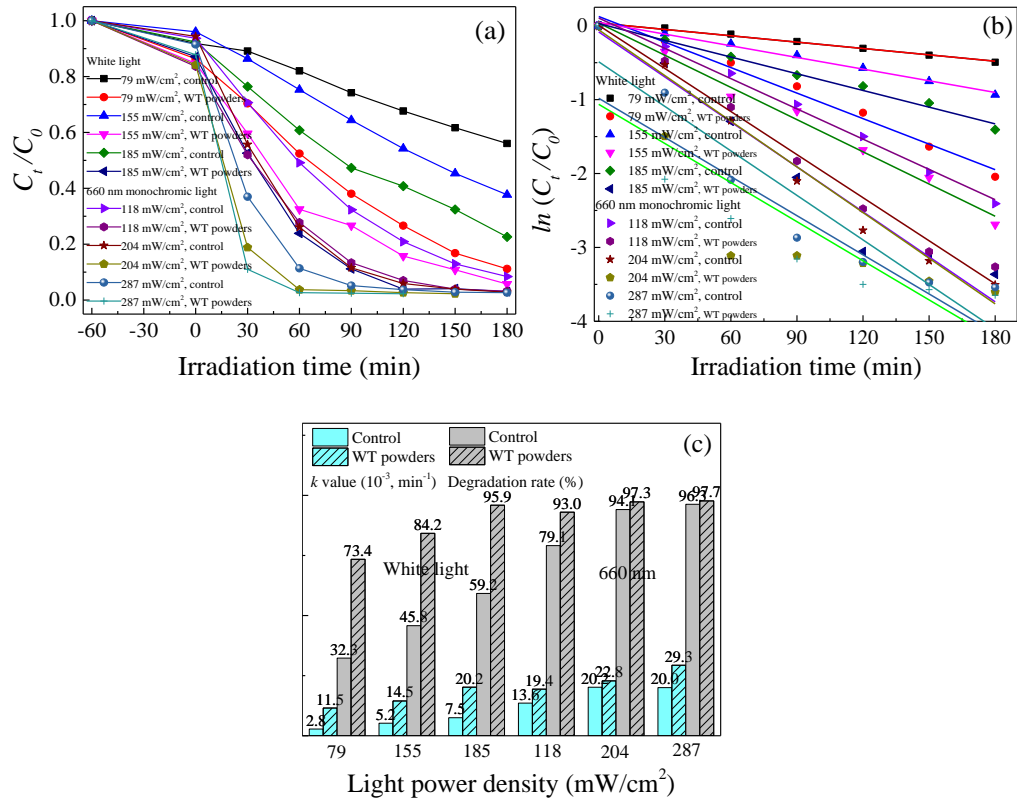


**Figure S4.** Photo-degradation of MB dye solution exposed to white light at the light power densities of 79, 155, and 185  $\text{mW/cm}^2$ , and exposed to 660 nm monochromic light at the light power densities of 118, 204, and 287  $\text{mW/cm}^2$  for 180 min, respectively

#### S7. Effect of the photocatalyst dosage

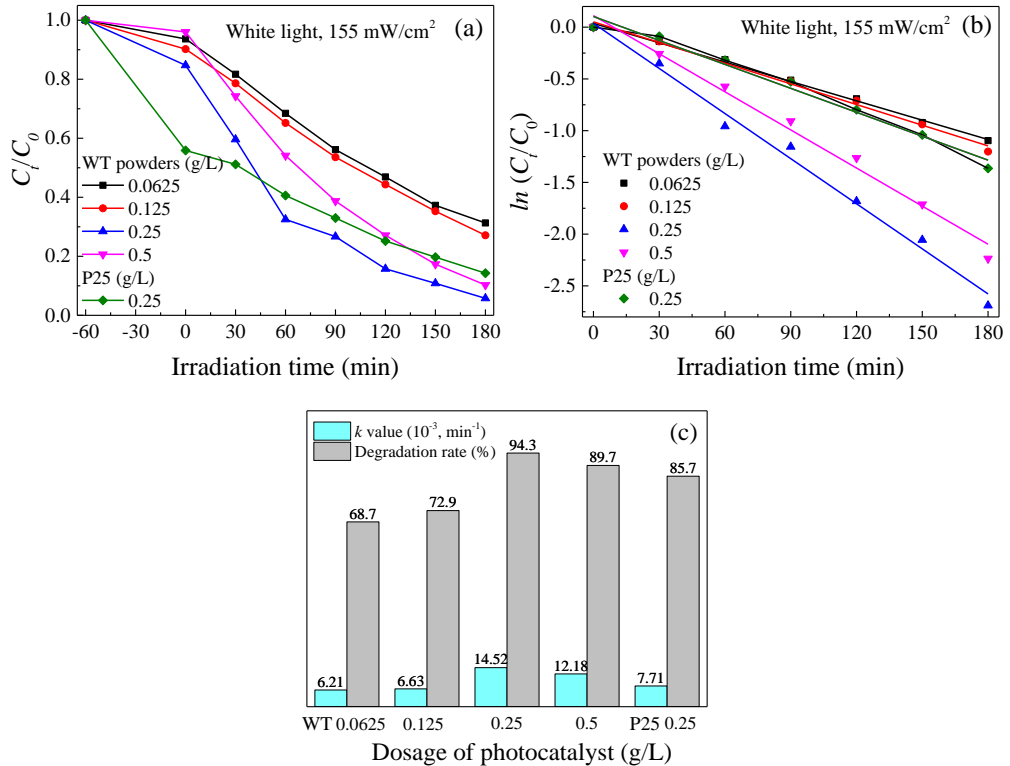


**Figure S5.** Photo-degradation of MB dye solution by different dosages of WT powders under 155  $\text{mW/cm}^2$  white light irradiation for 180 min

#### S8. Effect of the initial dye concentration

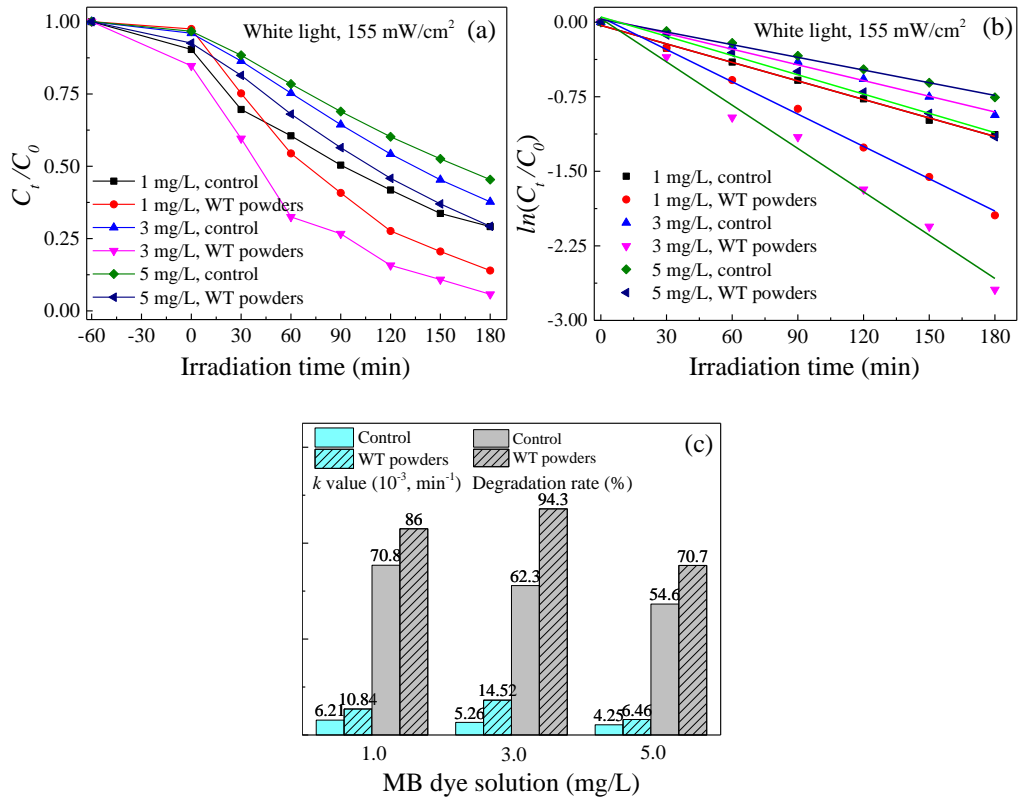


**Figure S6.** Photo-degradation of MB dye solution with the concentrations of 1, 3, and 5 mg/L exposure to white light at the light power density of  $155 \text{ mW/cm}^2$  for 180 min

### S9. Effect of the pH value of solution

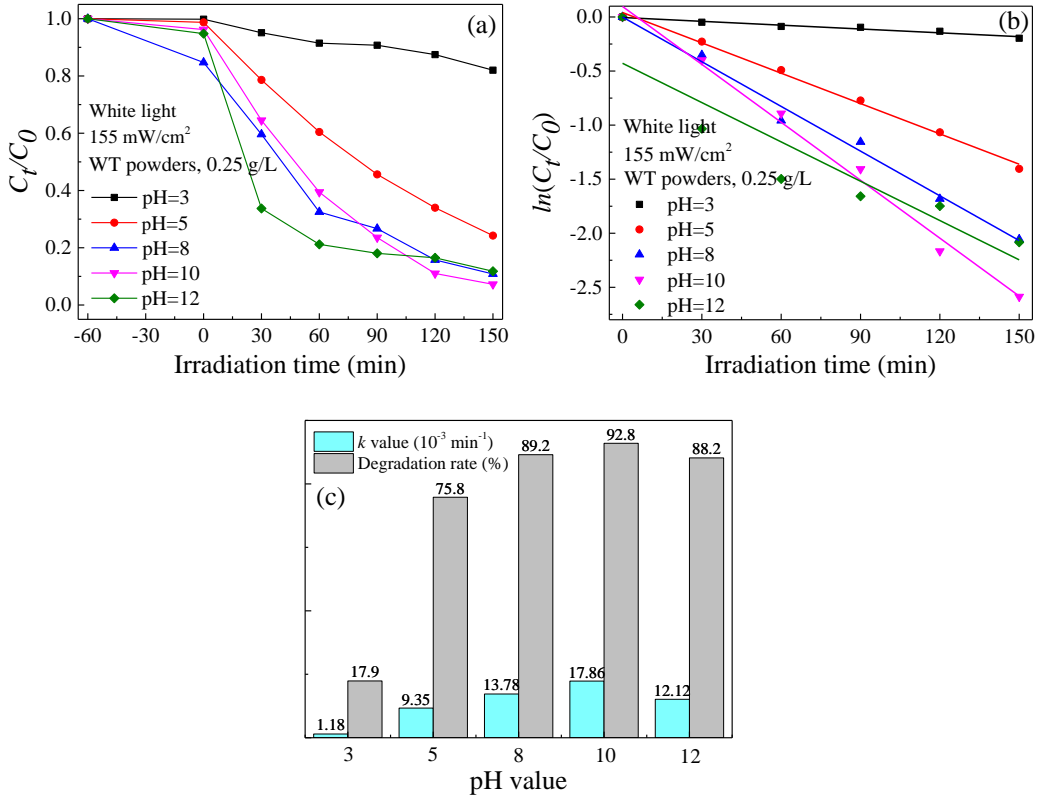


**Figure S7.** Effect of the pH value of dye solution on the photo-degradation efficiency of MB dye exposed to white light at the light power density of  $155 \text{ mW/cm}^2$  for 150 min

### S10. Effect of the oxidant agent $\text{H}_2\text{O}_2$

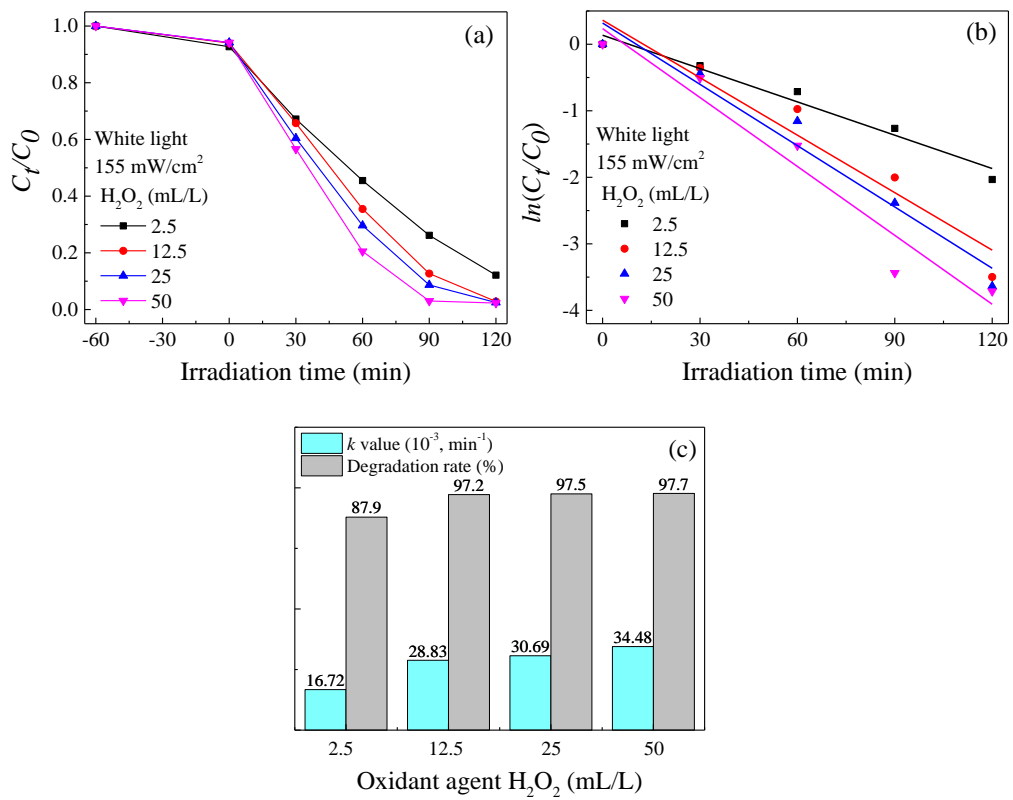


**Figure S8.** Effect of the co-catalyst  $\text{H}_2\text{O}_2$  on the photo-degradation efficiency of MB dye solution exposed to white light at the light power density of  $155 \text{ mW/cm}^2$  for 120 min

### S11. Effects of air and $\text{N}_2$

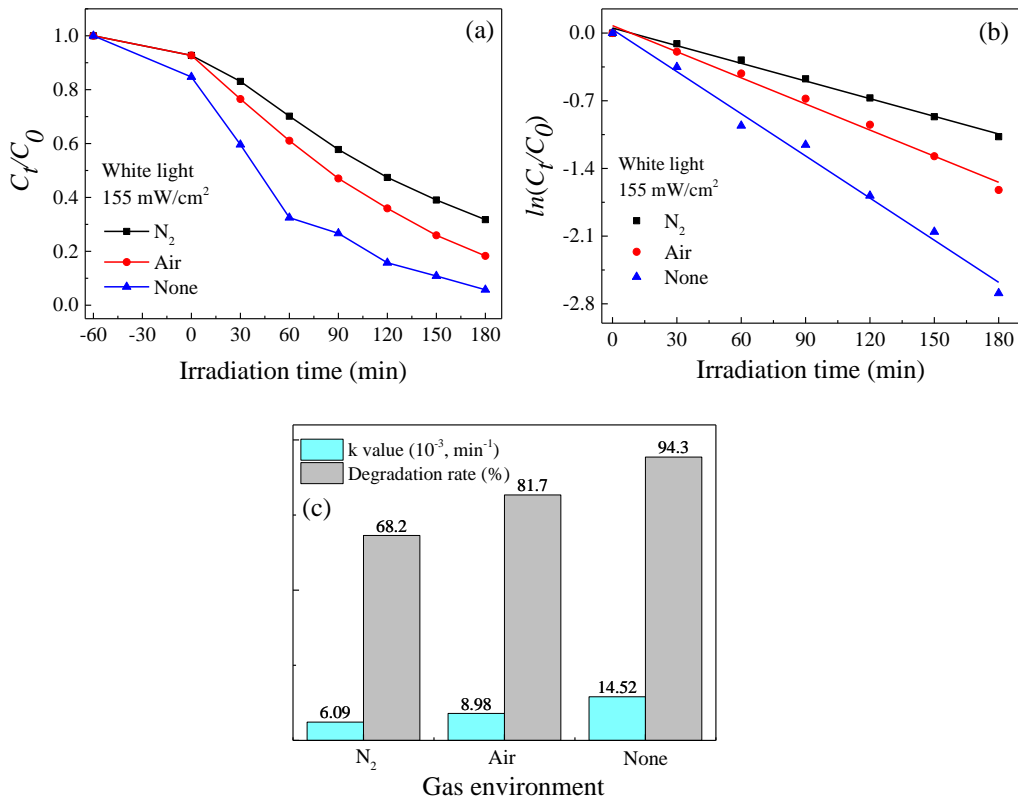


**Figure S9.** Effect of a gas environment on the photo-degradation efficiency of MB dye solution exposed to white light at the light power density of  $155 \text{ mW/cm}^2$  for 180 min

### S12. Comparison of the photo-degradation efficiency of MB dye solution by the WT powders

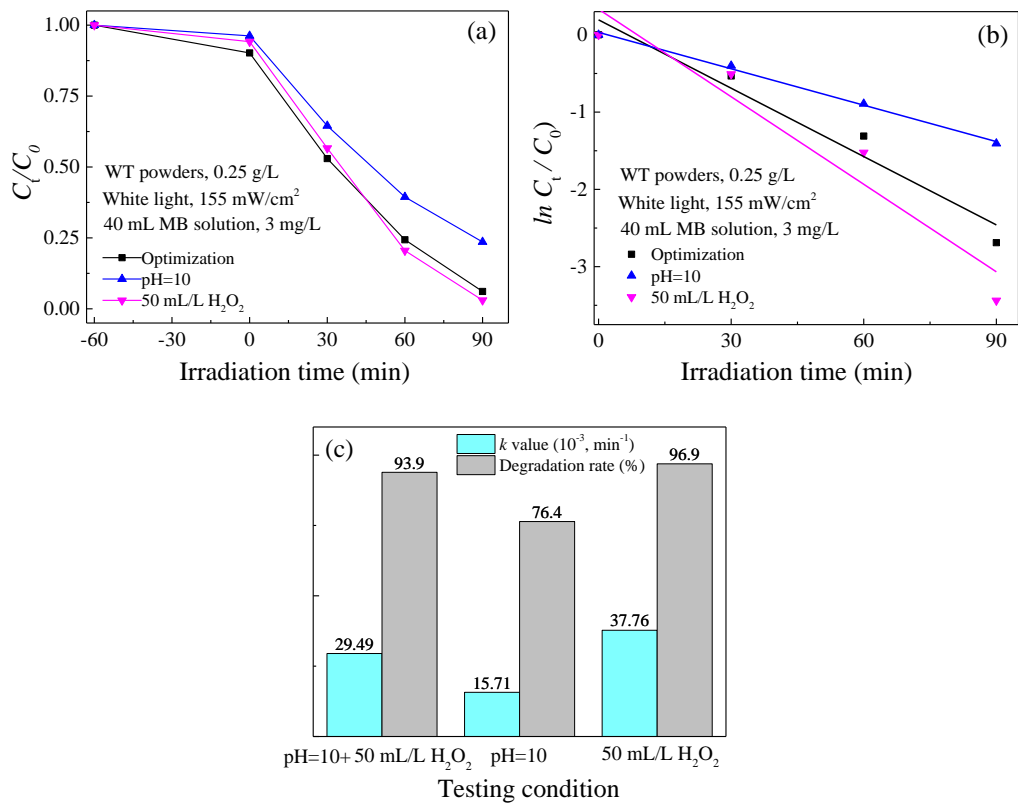


**Figure S10.** Comparison of photo-degradation efficiency of MB dye solution under different testing conditions for 90 min

### S13. Comparison of photo-degradation of different types of dyes by the WT powders

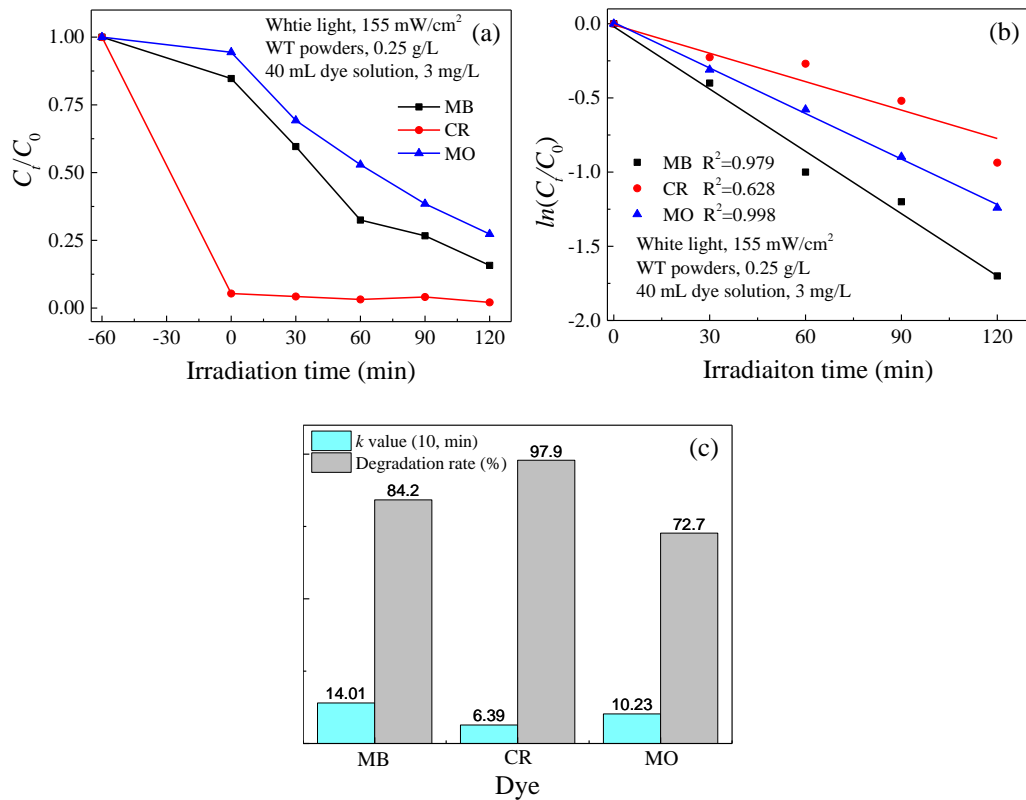


**Figure S11.** Comparison of photo-degradation of MB, CR and MO dye solution by the WT powders under 155 mW/cm<sup>2</sup> white light irradiation for 120 min

### S14. Reusability and stability of the WT powders

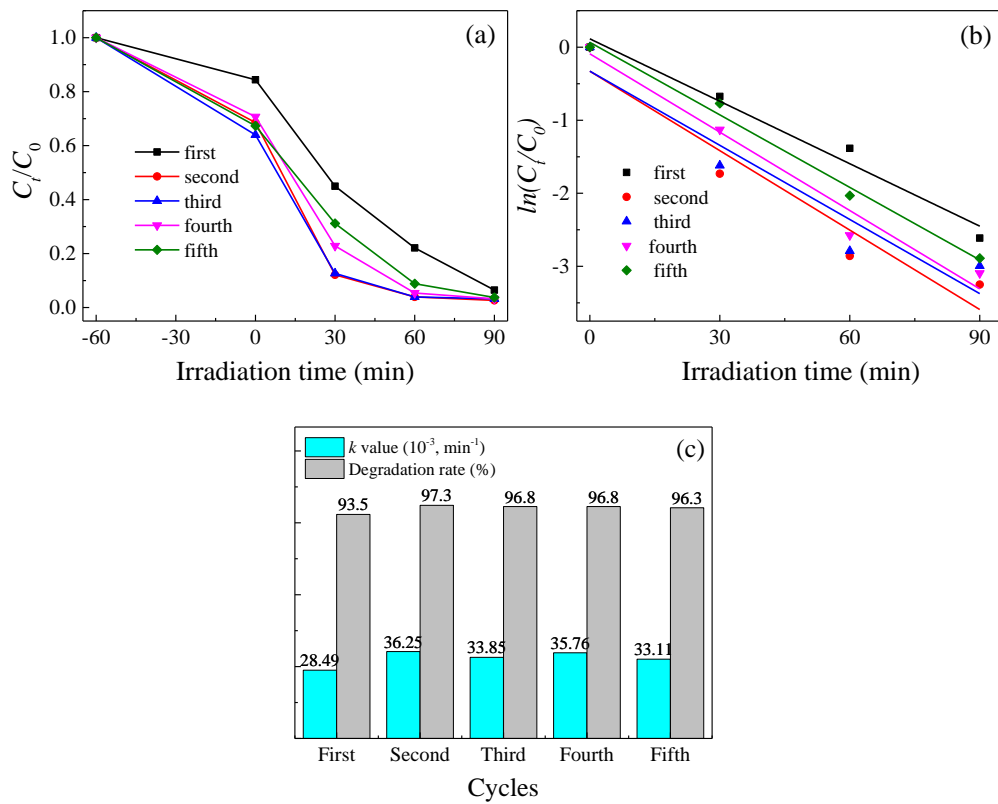


**Figure S12.** Recycle photo-degradation of MB dye solution by the WT powders under  $155 \text{ mW/cm}^2$  white light irradiation for 90 min

### S15. The trapping experiments for photo-degradation of MB dye solution

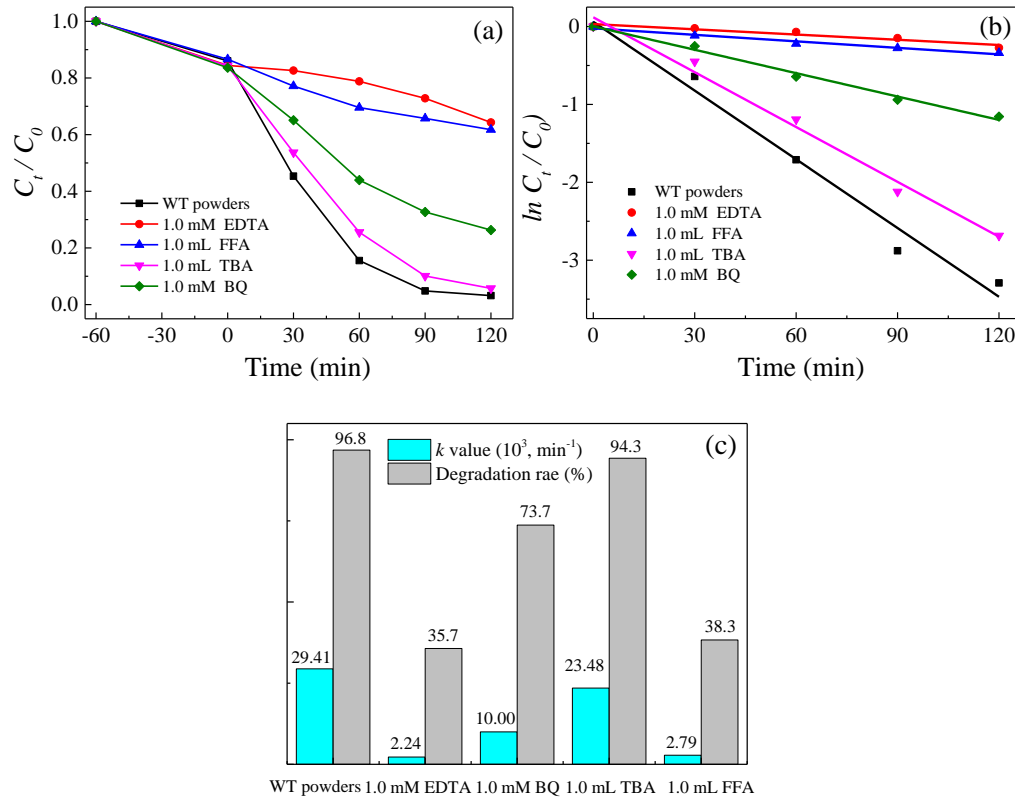


**Figure S13.** Trapping experiments for photo-degradation of MB dye solution by the WT powders by adding 1.0 mM EDTA, 1.0 mM BQ, 1.0 mL TBA, and 1.0 mL FFA, respectively under  $155 \text{ mW/cm}^2$  white light irradiation for 120 min